Metabolic Pathways of Carcinogenic Chromium

Elena Gaggelli,[1] Francesco Berti,[1] Nicola D'Amelio,[1] Nicola Gaggelli,[1] Gianni Valensin,[1] Lucia Bovalini,[2] Alessandro Paffetti,[2] and Lorenza Trabalzini[2]

[1]Department of Chemistry and the NMR Center, and [2]Department of Molecular Biology, Biochemistry Section, University of Siena,

The products of hexavalent chromium [Cr(VI)] reduction by glutathione (GSH) alone or in the presence of equimolar quantities of aspartate (Asp) and/or glutamate (Glu) and a chromium-containing material extracted from bovine liver were studied by ultraviolet–visible spectrum (UV-vis) studies, electrospray mass spectrometry (ES–MS), electron paramagnetic resonance (EPR), and nuclear magnetic resonance (NMR). Reduction of chromate by GSH was followed by UV-vis and NMR, revealing the formation of a paramagnetic complex in which GSH acts as a ligand. ES-MS and EPR measurements provided unequivocal evidence of a dimeric $Cr(V)_2GSH_2$ species in which the two metal ions are bridged by the γ-Glu carboxylate. The analysis of the ^1H and ^{13}C shifts experienced by GSH protons and the values of paramagnetic contributions to proton spin-lattice relaxation rates provided a set of constraints for structural determination. The same experiments were repeated in the presence of an equimolar concentration of Asp, revealing the formation of a dimeric Cr(V) paramagnetic complex in which the two metals are now bridged by Asp. Nuclear magnetic resonance dispersion profiles show that water is not displaced by Asp and that the correlation time of this complex is slowed by the increased complexity. When Glu is also included in the solution in equimolar concentration to GSH and Asp, data are consistent with the formation of many mono- and dinuclear species, with the three ligands competing with each other. Finally, the spectroscopic investigation of the chromium-containing material extracted from bovine liver revealed the presence of a complicate mixture of Cr(IV) or Cr(V) complexes, among which some Cr(V)–GSH species are present alone or with other ligands in the metal coordination sphere. ***Key words:*** **Asp, chromium, electron paramagnetic resonance, electrospray mass spectrometry, Glu, glutathione, LMWCr, nuclear magnetic resonance, ultraviolet–visible spectrum.** ***Environ Health Perspect*** **110(suppl 5):733–738 (2002).**
http://ehpnet1.niehs.nih.gov/docs/2002/suppl-5/733-738gaggelli/abstract.html

Human exposure to hexavalent chromium compounds has been firmly linked with the induction of cancer (*1,2*). Chromate, or dichromate, in fact, easily enters cells through the sulfate channel (*3*) and is quickly reduced by glutathione (GSH) (*4*), ascorbic acid (*4*), or cysteine (Cys) (*4,5*). In exposed animals, the ultimate step of the metabolic pathway yields Cr(III) inserted within the cell nucleus, where it cross-links DNA to proteins (mainly actin) or GSH (*6,7*). The intermediate steps have not been thoroughly characterized so far, although Cr(V) and Cr(IV) compounds have been demonstrated to produce reactive oxygen species, thiyl, and carbon-based radicals (*8–12*).

Despite such toxic features, Cr(III) is essential in mammals that require it for normal carbohydrate and lipid metabolism (*13–15*). Since the so-called glucose tolerance factor failed to be chemically characterized (*16*), chromium tris-picolinate [$Cr(pic)_3$] has been proposed as the biologically active form of Cr(III) and extensively commercialized (*17–19*). In the early 1980s a new chromium-binding oligopeptide, named "low-molecular-weight chromium" (LMWCr) (*15,20–31*), also known as chromodulin (*32*), was isolated in tissues, mainly in the liver, of several mammals (*24*). Moreover, the use of $Cr(pic)_3$ as a dietary supplement has been challenged by its proven features of *a*) catalytically producing hydroxyl radicals and *b*) being potentially mutagenic as are all other Cr(III) compounds (*33*).

LMWCr has been investigated extensively for its chemical and biological features (*28,29,34*):

- The protein is isolated with the best yield from bovine liver, with few separation procedures (10–30 mg of protein from 1 kg of diced liver).
- Ultraviolet–visible spectrum (UV-vis), electron paramagnetic resonance (EPR), and nuclear magnetic resonance (NMR) features suggest the presence of a peptide-bound cluster of four oxo-bridged octahedral Cr(III) ions.
- The protein *a*) increases the ability of rat adipocytes to metabolize glucose (in the presence of insulin); *b*) stimulates glucose metabolism in a way proportional to its chromium contents; and *c*) does not change the concentration of insulin required for half-maximal stimulation.
- The average molecular weight is approximately 1.5 kDa.
- The protein is composed of only four amino acids [glutamate (Glu), aspartate (Asp), glycine (Gly), Cys] in the average ratio Glu:Asp:Gly:Cys = 2.15:4.47:2.47:2.35.
- The apo-protein may be generated (*29*), but no delineation has been provided of its chemical and spectroscopic features.

All these, and other properties (*35*), are therefore flawed by the impossibility of determining the primary sequence of the protein (*29*).

We also considered that the reported composition of LMWCr roughly corresponds to two GSH, two Asp, and two Glu molecules, and that the intermediate steps of metabolic reduction of Cr(VI) are worth further investigation.

For these two reasons, we present our spectroscopic UV-vis, electrospray mass spectrometry (ES-MS), and EPR and NMR studies of *a*) the products of Cr(VI) reduction by GSH alone or in the presence of equimolar quantities of Asp and/or Glu, and *b*) the chromium-containing material extracted from bovine liver.

A first report of some preliminary results has been published elsewhere (*36*).

Materials and Methods

All chemicals were obtained from Sigma Chemical Co. (Milano, Italy) and used without further purification. The extraction of the chromium-containing material from the bovine liver was performed by exactly following the already published protocol (*29*). Solutions were obtained in deuterium oxide buffered at pH 7.4 and deoxygenated by freeze–thaw cycles.

NMR spectra were obtained on 4.7, 11.7, 14.1, and 18.8 T Bruker NMR spectrometers (Bruker, Rheinstetten/Karlsruhe, Germany) at temperatures controlled at ± 0.2 K. Chemical shifts were referenced to external tetramethylsilane. COSY (correlation spectroscopy), TOCSY (total correlation spectroscopy), NOESY (nuclear Overhauser effect spectroscopy), and ROESY (rotating frame Overhauser effect spectroscopy) two-dimensional experiments were performed by using standard sequences. While TOCSY and COSY relate through bonds-coupled nuclei, NOESY and ROESY relate nuclei close in

This article is part of the monograph *Molecular Mechanisms of Metal Toxicity and Carcinogenicity.*

Address correspondence to G. Valensin, Dept. of Chemistry and the NMR Center, University of Siena, Via A. Moro, Siena 53100, Italy. Telephone: 39-0577-234231. Fax: 39-0577-234254. E-mail: valensin@unisi.it

Received 3 February 2002; accepted 3 June 2002.

space coupled via dipolar interaction. Spin-lattice relaxation rates were measured with inversion recovery pulse sequences and calculated by exponential regression analysis of the decay curves of longitudinal magnetization components.

UV-vis absorption spectra were taken on an HP 8453 spectrometer (Hewlett Packard, Palo Alto, CA, USA) equipped with the HP UV-vis Chemstation software (Hewlett Packard 95-98, Rev.A.06.04[48]). Quartz cells with a 1.0-cm path length were used.

X-band EPR spectra were acquired on a Bruker 200D SRC spectrometer (Bruker) at temperature = 298 ± 0.5 K. Microwave frequencies were measured with an XL Microwave 3120 counter (Jagmar, Krakow, Poland). The spectrometer was interfaced with a PS/2 Technical Instruments Hardware computer, and the data were acquired using the EPR data system CS-EPR, produced by Stelar Inc. (Mede, Italy). The spectra were preliminarily corrected for baseline drift. EPR spectra at 282 GHz were acquired under the following conditions: temperature = 10 K, microwave frequency = 282 GHz, field modulation frequency = 9.50 kHz, modulation amplitude = 40 mA, time constant = 3 s, sweep rate = 0.3 T/min. The simulated spectrum was calculated by using a program written by Weihe described in Jacobsen et al. (*37*). For two unpaired electrons considered as point dipoles, the following formula can be applied (*38*):

$$D = -\frac{3g^2\beta}{2\langle r \rangle^3} \qquad [1]$$

where D is one of the parameters for zero field splitting (the other, E, is zero). This formula yields $D = -0.0811$ cm^{-1} when the two dipoles are 0.414 nm apart. The other parameter for the simulation was the single-crystal EPR line width taken at 100 mT.

ES–MS spectra were recorded with a Perkin Elmer Sciex triple quadrupole liquid chromatography/mass spectrometry/mass spectrometry (LC/MS/MS) with a water/formic acid (equilibrated at pH 7.4) mobile phase. The ion at m/z 717 was selected and passed through a collision cell into a second mass analyzer.

Molecular structures were generated by the HYPERCHEM software package (*39*) implemented on a Pentium 120-MHz PC by using the Huckel semi-empirical method for charge calculations and the MM+ force field for molecular mechanics and dynamics calculations (*39*).

Results and Discussion

The reduction of chromate by GSH at pH 7.4 was first investigated by UV-vis spectroscopy (Figure 1). As previously noted (*4*), the progressive disappearance of the chromate absorption at approximately 345 nm was accompanied by the appearance of a strong broad absorption centered at 435 nm and attributed to a Cr(VI)–thioester species (*40*). That this last is a transient species is clearly demonstrated by the kinetic plot shown in Figure 2: within the first 10–15 min, it has almost disappeared and only a strong absorption in the UV region at approximately 206 nm is left, suggesting exclusive formation of Cr(V) or Cr(IV) species (*4*).

NMR spectra, recorded at 14.1 T on a solution containing GSH and GSSG (the oxidized form of GSH) at a ratio of 5:1 (pH 7.4) upon progressive addition of sodium chromate (Figure 3), allowed us to make relevant inferences on the formed species. The relevant resonances are labeled in Figure 3 and are related to the chemical formulas in Figure 4. The spectra clearly demonstrate formation of GSSG at the expense of GSH. Lowering and raising, respectively, of the intensities of well-separated lines is in fact observed. However, the extensive broadening and the upfield shift experienced by resonances belonging to GSH indicate the formation of a paramagnetic complex in which GSH acts as a ligand. In fact, both ^{1}H and ^{13}C-NMR chemical shifts were selectively affected, and proton spin-lattice relaxation rates were selectively enhanced (Figures 5, 6).

Assignment of binding donors of GSH was based on analysis of NMR parameters yielding the following evidence:

- Cys H_α, γ-Glu H_α, γ-Glu H_β, and γ-Glu H_γ were the most upfield-shifted GSH ^{1}H signals upon addition of chromate.
- All proton spin-lattice relaxation rates were consistently enhanced, with protons within the Cys and Glu moieties being more affected than those of Gly.
- Cys C_α, γ-Glu C_α, and γ-Glu C_β were the most affected GSH ^{13}C signals upon addition of chromate.

Both the change in chemical shifts and the enhancement of relaxation rates are larger at closer distances from the metal center that provides dipolar and hyperfine local fields at the nearby nuclei (*41,42*).

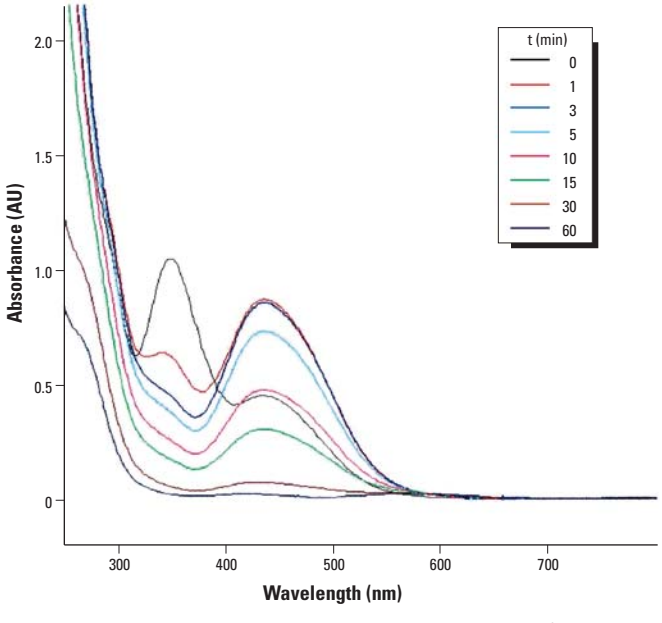

Figure 1. UV-vis spectra of sodium chromate solution at pH 7.4 (temperature = 300 K) as a function of time (*t*) after the addition of GSH.

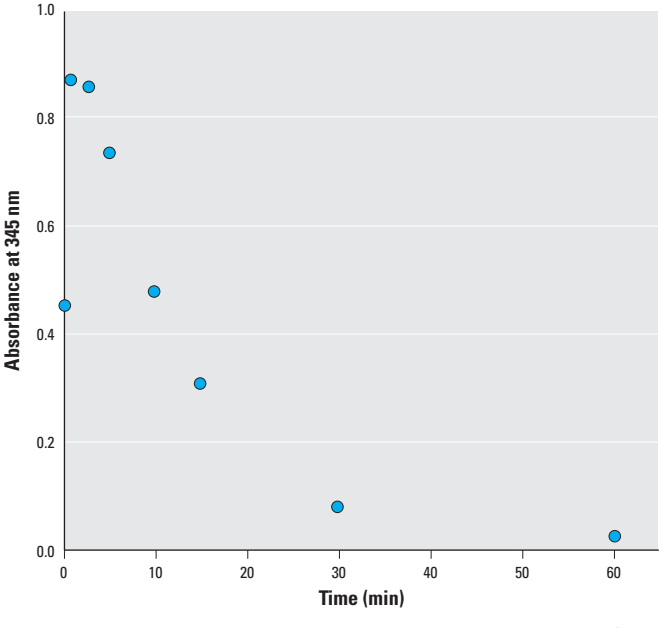

Figure 2. Absorbance at 435 nm of sodium chromate solution at pH 7.4 (temperature = 300 K) as a function of time after the addition of GSH.

The dipolar contribution to the chemical shift relies on a large value of the anisotropy of magnetic susceptibility (*42*), which does not manifest in EPR spectra. Only the contact contribution therefore needs to be considered, given by:

$$\Delta\delta = -\frac{A}{\hbar}\frac{g\mu_B S(S+1)}{3\gamma_N kT} \qquad [2]$$

where A is the contact coupling constant, $\hbar$ the reduced Planck's constant ($\equiv h/2\pi$), μ_B is the electron Bohr magneton, S is the total spin number, γ_N is the magnetogyric ratio, k is the Boltzmann constant, and T is temperature. This equation states that an electron spin magnetic moment determines the shift of coupled nuclear resonances. The size of the shift experienced by any nuclear spin in a given metal complex is therefore determined by A, which in turn is proportional to the unpaired electron spin density at the nucleus.

On the other hand, the relatively long electron relaxation times expected for $S = 1/2$ metal ions (*41,42*) make the contact contribution to nuclear spin-lattice relaxation negligible. The longitudinal relaxation rate of a nucleus sensing the electron magnetic moment can therefore be approximated by the dipole–dipole interaction, as described by Solomon (*43*). Solomon's equation considers the dipole–dipole interaction of nuclear and electron magnetic moments at a certain distance r from each other. The obtained relaxation rate is determined by the squared dipole–dipole interaction energy that is modulated by molecular tumbling in solution. The mathematical expression is (*43*)

$$R_{1M} = \left(\frac{\mu_o}{4\pi}\right)^2 \frac{\gamma_n^2 g^2 \mu_B^2 S(S+1)}{r^6} \left\{\frac{3\tau_c}{1+\omega_H^2\tau_c^2} + \frac{7\tau_c}{1+\omega_e^2\tau_c^2}\right\} \qquad [3]$$

where μ_o is vacuum permeability, ω_H and ω_e are the proton and electron Larmor frequencies, τ_c is the motional correlation time, and r is the proton–metal distance. The isotropic hyperfine coupling of the unpaired electron with the metal nuclear spin modifies the Solomon equation (*44*); moreover, the Curie mechanism (*42*) is likely to contribute the nuclear relaxation pathway at the high magnetic field used. However, the dependence upon the inverse of r to the sixth power is maintained in any case. As a consequence, a large relaxation rate enhancement indicates spatial proximity of the paramagnetic center to the corresponding proton.

NMR data therefore support the exclusion of Cys sulfhydryl and Gly carboxylate from the possible donor set to the paramagnetic chromium ion.

The results obtained by ES–MS and EPR (both at 9.5 and 282 GHz) provided unequivocal evidence of the predominance of a dimeric $Cr(V)_2GSH_2$ species (*36*) in which the two metal ions are bridged by the γ-Glu carboxylate, as confirmed by the structure of several polynuclear chromium complexes (*34*). Structural details of this cluster are shown in Figure 7; it is apparent that the γ-Glu amino and the γ-Glu amide groups complete the coordination donor set to chromium (*36*).

Repetition of the same experiments in the presence of Asp at a concentration equimolar to GSH yielded the following evidence:

- ^{1}H-NMR signals of GSH and Asp are both affected by reduced chromate, and the

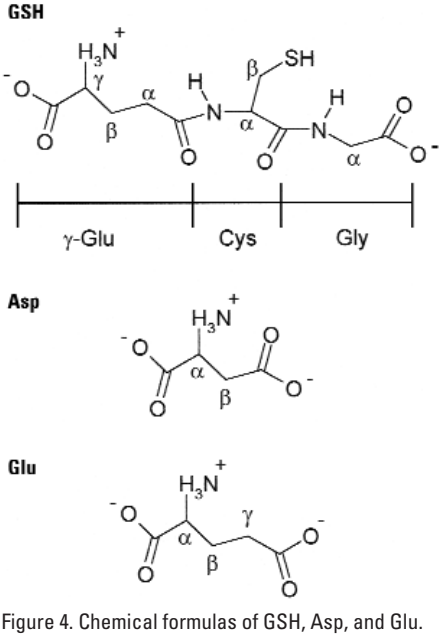

Figure 4. Chemical formulas of GSH, Asp, and Glu.

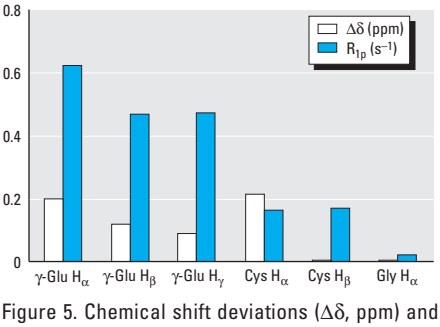

Figure 5. Chemical shift deviations (Δδ, ppm) and paramagnetic contributions to spin-lattice relaxation rates (R_{1p}, s^{-1}) of GSH protons (16.7 mM) in the presence of sodium chromate (5 mM, temperature = 300 K).

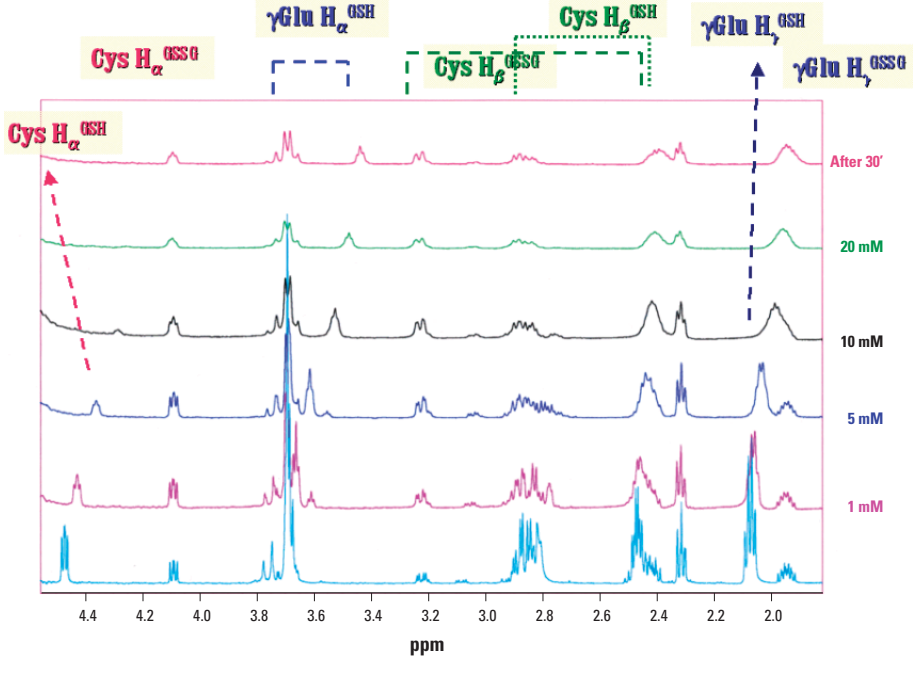

Figure 3. ^{1}H-NMR spectra of a solution of GSH (16.7 mM) and GSSG (3.3 mM) in heavy water (D_2O; pH 7.4, temperature = 300 K) (bottom) upon addition of sodium chromate 1, 5, 10, and 20 mM (from bottom to top). The spectrum on top was recorded 30 min after the last step of the titration.

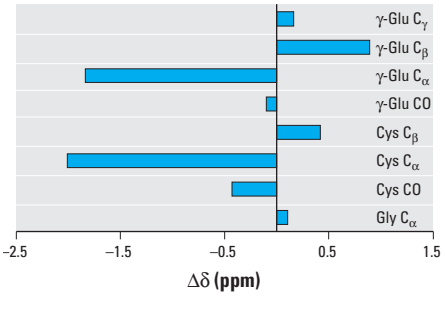

Figure 6. Chemical shift deviations (Δδ, ppm) of GSH carbons (16.7 mM) in the presence of sodium chromate (5 mM, temperature = 300 K).

relaxation enhancements of GSH are further enhanced (Figure 8).
- EPR spectra indicate occurrence of a similar species with the same electronic *g* factor value and slightly broader signals (Figure 9).
- NOESY spectra give evidence of cross-peaks between Asp protons and GSH protons, indicating that both participate in metal binding (Figure 10A).
- ^{1}H-NMR dispersion curves of water protons (Figure 11) demonstrate that water bound to paramagnetic chromium in the $Cr(V)_2GSH_2$ species is not displaced by Asp, with consequent decrease in the relaxivity. On the contrary, relaxation rates of water protons are further enhanced, thus indicating that, most probably the correlation time has slowed in the presence of Asp, which enhances the molecular complexity.

We therefore conclude that both Asp and GSH bind chromium in a dimeric $Cr(V)_2GSH_2Asp_2$ complex, the structure of which was indeed solved by molecular mechanics and dynamics restrained by constraints obtained from NMR data (Figure 12). It turns out that the two Cr(V) ions are now bridged by Asp, which lets them reach a Cr–Cr distance of 0.343 nm to be compared with the Cr distance found for the $Cr(V)_2GSH_2$ complex (0.414 nm). This shortened distance is consistent with the broader EPR lines and, taken together with the increase in molecular complexity, also with the Asp-induced enhancement of proton relaxation rates of either GSH or bound water.

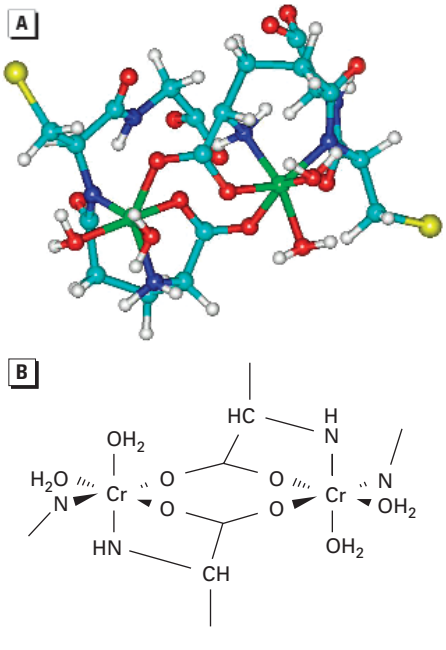

Figure 7. (*A*) Stick model of dimeric $Cr(V)_2GSH_2$ complex as determined by NMR and EPR constraints. Coloring scheme: chromium, green; oxygen, red; carbon, cyan; hydrogen, light gray; nitrogen, blue; sulfur, yellow. (*B*) Details of the Cr–Cr cluster.

When Glu was also included in the solution mixture exposed to chromate additions in equimolar concentration with both GSH and Asp, the following results were obtained:
- ^{1}H-NMR signals of GSH, Asp and Glu were all affected by reduced chromate, but the relaxation enhancements of GSH and Asp are somehow reduced (Figure 8).
- No GSH–Glu or Asp–Glu cross-peaks are detectable in NOESY spectra, in which the GSH–Asp connectivities are washed out also (Figure 10B).
- ^{1}H-NMR dispersion curves of water protons (Figure 11) demonstrate that Glu almost completely destroys the enhancement induced by Asp, such that occurrence

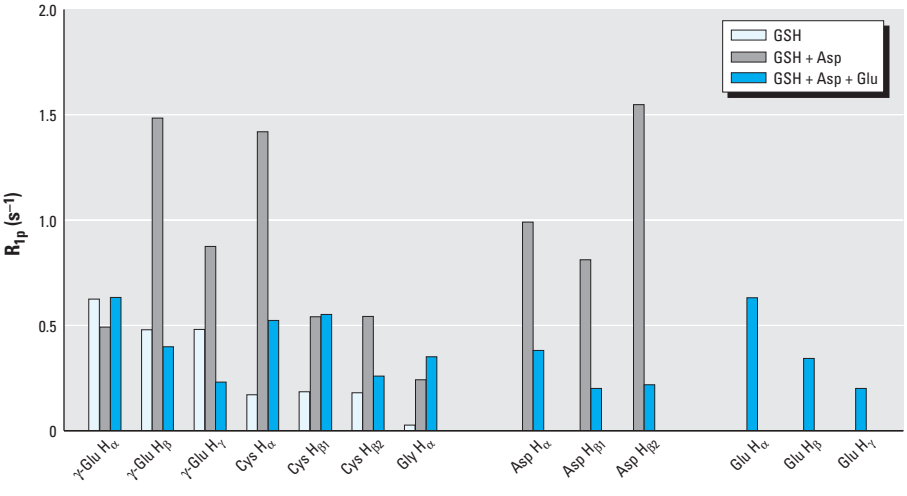

Figure 8. Paramagnetic contributions to proton spin-lattice relaxation rates R_{1p} (s^{-1}) of a 5-mM solution of sodium chromate in the presence of GSH, GSH + Asp, and GSH + Asp + Glu (16.7 mM each; temperature =300 K).

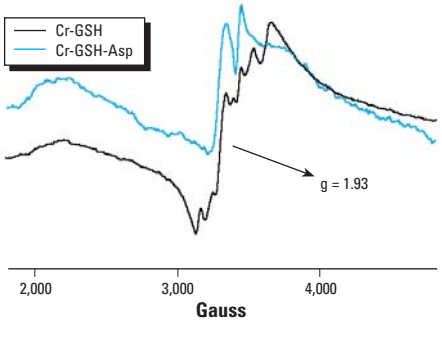

Figure 9. X-band EPR spectra of a solution of sodium chromate and GSH in the absence (black) and presence (blue) of Asp (temperature = 298 K).

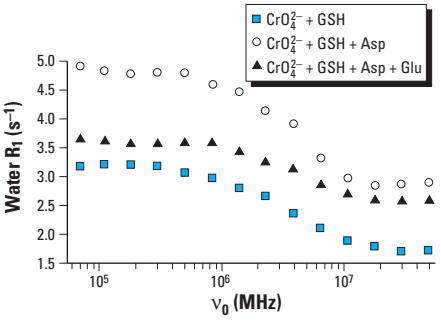

Figure 11. ^{1}H-NMR dispersion curves (R_1 vs ν_0) of water protons of a 5 mM solution of sodium chromate in the presence of GSH, GSH + Asp, and GSH + Asp + Glu (16.7 mM each; temperature = 300 K).

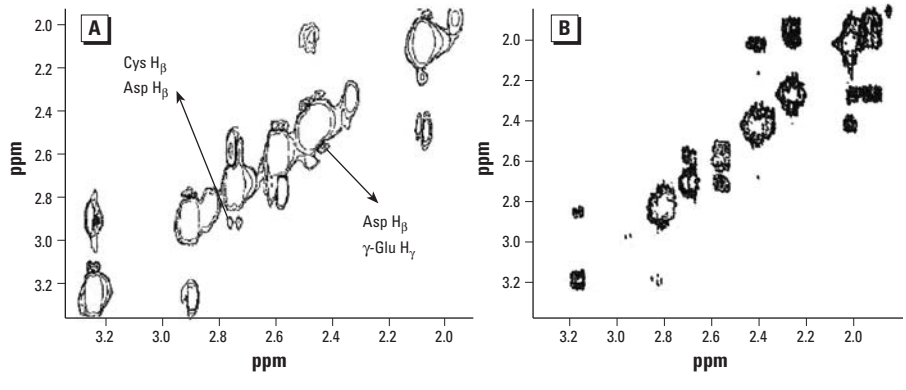

Figure 10. Selected regions of NOESY spectra of a solution of sodium chromate, GSH, and Asp in the absence (*A*) and in the presence (*B*) of Glu.

of GSH, Asp, and Glu in the same metal complex can be reasonably excluded.

We therefore conclude that Glu, Asp, and GSH compete with each other for chromium, with the possible simultaneous formation of many mono- and dinuclear species. Although GSH alone or together with Asp succeeds in clustering chromium, the three ligands together do not cluster chromium and give rise to complex equilibria in solution.

The material extracted from bovine liver was finally investigated. Although the already published protocol (*29*) was exactly followed and repeated 3 times, what we found was quite different from the published features of LMWCr (*28,29,34*):

- UV-vis spectra (Figure 13) are very similar to those obtained in the GSH/GSSG mixture upon addition of chromate at pH 7.4 and exclude whatever possibility of having Cr(III) in the solution.
- ES–MS spectra (Figure 14) exclude the occurrence of detectable species at $m/z > 786.4$.
- The first recorded NMR spectrum (Figure 15A) is consistent with a very broad paramagnetic signal that superimposes to a well-resolved diamagnetic region. Moreover, a down-shifted broad signal at +65 ppm appears that somewhat resembles the one observed with LMWCr (*29*). However, the spectrum obtained at higher frequency (Figure 15B) with an NMR "old-fashioned" probe (without gradients) reveals that this feature is an artifact; on the contrary, some features do appear in the upfield-shifted region (–20 ↔ –40 ppm). These findings confirm the absence of Cr(III) and indicate the occurrence of paramagnetic Cr(IV) or Cr(V) compounds.
- The EPR spectrum (Figure 16) is again very similar to that obtained in the GSH/GSSG mixture upon addition of chromate.

All the obtained results indicate that what we have extracted from bovine liver is a complicate mixture of Cr(V) complexes, among which some Cr(V)–GSH species are present alone or with other ligands in the metal coordination sphere.

We conclude that what we have investigated so far suggests that GSH not only is a primary target for oxidation by chromate but also acts as an efficient ligand stabilizing Cr(V) in a dimeric bridged cluster. When Asp is also present in the medium, it may act as an additional ligand to Cr(V) with formation of a new type of dinuclear cluster. If Asp and Glu are both present in the medium, together with GSH, the three ligands compete for the metal and a complicate mixture of species in equilibrium is observed. It is worth emphasizing that what we obtain by reducing chromate *in vitro* with GSH, GSH + Asp, or GSH + Asp + Glu represents a good model for the mixture of species that is detected when dichromate, added to homogenized liver in the first step of the extraction of LMWCr (*29*), is reduced and complexed by endogenous ligands occurring in the cell cytoplasm.

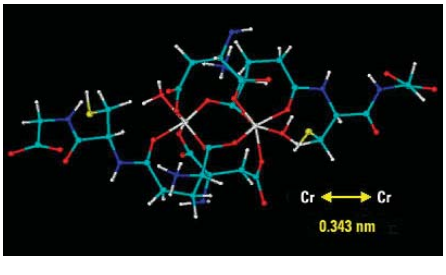

Figure 12. Stick model of dimeric $Cr(V)_2GSH_2Asp_2$ complex as determined by NMR structural constraints. Coloring scheme: chromium, white; oxygen, red; carbon, cyan; hydrogen, light gray; nitrogen, blue; and sulfur, yellow.

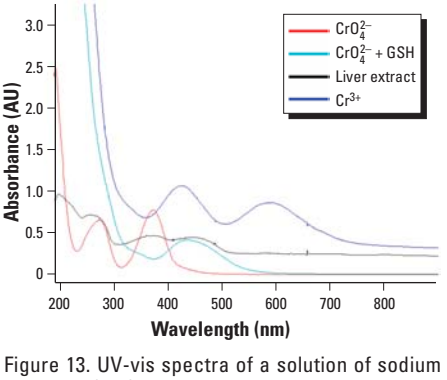

Figure 13. UV-vis spectra of a solution of sodium chromate (red), sodium chromate in the presence of GSH (cyan), the material extracted from liver (black), and Cr(III) (blue) (temperature = 300 K).

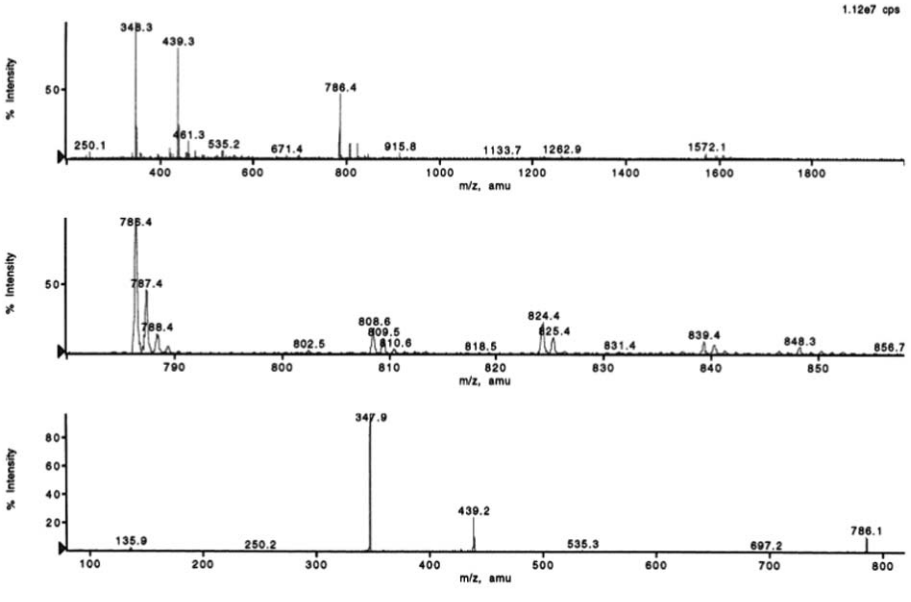

Figure 14. Regions of ES–MS spectrum of the material extracted from liver.

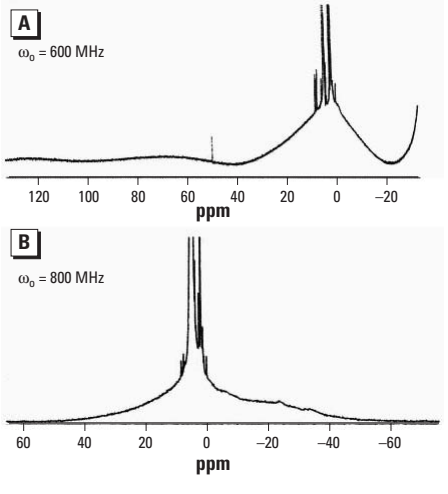

Figure 15. ^{1}H-NMR spectra of the material extracted from liver recorded at (*A*) 600 MHz and (*B*) 800 MHz (temperature = 300 K).

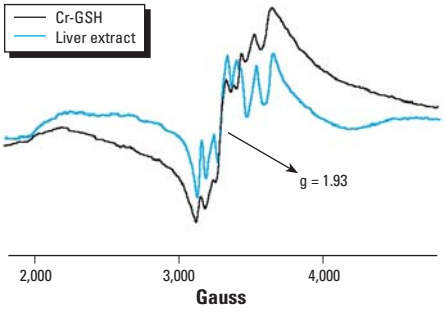

Figure 16. X-band EPR spectra of chromium–GSH complex (black) and the material extracted from liver (blue) (temperature = 298 K).

References and Notes

1. Hamilton JW, Wetterhahn KE. Chromium (VI)-induced DNA damage in chick embryo liver and blood cells *in vivo*. Carcinogenesis 7:2085–2088 (1986).
2. Kozlowski H, Swiatek J, Bal W. Chemical bases of metal induced mutagenesis and carcinogenesis. In: Education in Advanced Chemistry. Vol 3: Environmental Chemistry and Protection (Marciniec B, Ziolkowski JJ, eds). Wroclaw:Poznan, 1996;41–60.
3. Wiegand HJ, Ottenwälder H, Bolt HM. Recent advances in biological monitoring of hexavalent chromium compounds. Sci Total Environ 71:309–315 (1988).
4. Connett PH, Wetterhahn KE. *In vitro* reaction of the carcinogen chromate with cellular thiols and carboxylic acids. J Am Chem Soc 107:4282–4288 (1985).
5. Kwong DWJ, Pennington DE. Stoichiometry, kinetics, and mechanisms of the chromium(VI) oxidation of L-cysteine at neutral pH. Inorg Chem 23:2528–2532 (1984).
6. Miller CA III, Cohen MD, Costa M. Complexing of actin and other nuclear proteins to DNA by *cis*-diamminedichloroplatinum(II) and chromium compounds. Carcinogenesis 12:269–276 (1991).
7. Voitkun V, Zhitkovich A, Costa M. Cr(II)-mediated crosslinks of glutathione or amino acids to the DNA phosphate backbone are mutagenic in human cells. Nucleic Acids Res 26:2024–2030 (1998).
8. Kawanishi S, Inoue S, Sano S. Mechanism of DNA cleavage induced by sodium chromate(VI) in the presence of hydrogen peroxide. J Biol Chem 261:5952–5958 (1986).
9. Shi X, Dalal NS. On the mechanism of the chromate reduction by glutathione: ESR evidence for the glutathionyl radical and an isolable Cr(V) intermediate. Biochem Biophys Res Commun 156:137–142 (1988).
10. Shi X, Dalal NS. On the hydroxyl radical formation in the reaction between hydrogen peroxide and biologically generated chromium(V) species. Arch Biochem Biophys 277:342–350 (1990).
11. Shi X, Dong Z, Dalal NS, Gannett PM. Chromate-mediated free radical generation from cysteine, penicillamine, hydrogen peroxide, and lipid hydroperoxides. Biochem Biophys Acta 1226:65–72 (1994).
12. Sugden KD, Wetterhahn KE. Direct and hydrogen peroxide-induced chromium(V) oxidation of deoxyribose in single-stranded and double-stranded calf thymus DNA. Chem Res Toxicol 10:1397–1406 (1997).
13. Anderson RA, Polansky MM, Bryden NA, Roginski EE, Mertz W, Glinsmann W. Chromium supplementation of human subjects: effects on glucose, insulin, and lipids variables. Metabolism 32:894–899 (1983).
14. Anderson RA. Nutritional factors influencing the glucose/insulin system: chromium. J Am Coll Nutr 16:404–410 (1997).
15. Davis MC, Vincent JB. Chromium oligopeptide activates insulin receptor tyrosine kinase activity. Biochemistry 36:4382–4385 (1997).
16. Toepfer EW, Mertz W, Polansky MM, Roginski EE, Wolf WR. Preparation of chromium-containing material of glucose tolerance factor activity from Brewer's yeast extracts and by synthesis. J Agric Food Chem 25:162–166 (1977).
17. Stearns DM, Armstrong WH. Mononuclear and binuclear chromium(III) picolinate complexes. Inorg Chem 31:5178–5184 (1992).
18. Evans GW, Bowman TD. Chromium picolinate increases membrane fluidity and rate of insulin internalization. J Inorg Biochem 46:243–250 (1992).
19. Anderson RA, Bryden NA, Polansky MM. Lack of toxicity of chromium chloride and chromium picolinate in rats. J Am Coll Nutr 6:273–279 (1997).
20. Yamamoto A, Wada O, Ono T. Isolation of a biologically active low-molecular-mass chromium compound from rabbit liver. Eur J Biochem 165:627–631 (1987).
21. Yamamoto A, Wada O, Manabe S. Evidence that chromium is an essential factor for biological activity of low-molecular-weight chromium binding substance. Biochem Biophys Res Commun 163:189–193 (1989).
22. Yamamoto A, Wada O, Suzuki H. Purification and properties of biologically active chromium complex from bovine colostrum. J Nutr 118:39–45 (1988).
23. Wada O, Wu GY, Yamamoto A, Manabe S, Ono T. Purification and chromium-excretory function of low molecular-weight, chromium-binding substances from dog liver. Environ Res 32:228–239 (1983).
24. Yamamoto A, Wada O, Ono T. Distribution and chromium-binding capacity of a low-molecular-weight, chromium-binding substance in mice. J Inorg Biochem 22:91–102 (1984).
25. Davis CM, Sumrall KH, Vincent JB. The biologically active form of chromium may activate a membrane phosphotyrosinephosphatase (PTP). Biochemistry 35:12963–12969 (1996).
26. Davis MC, Vincent JB. Chromium in carbohydrate and lipid metabolism. J Biol Inorg Chem 2:675–679 (1997).
27. Sumrall KH, Vincent JB. Is glucose tolerance factor an artifact produced by acid hydrolysis of low-molecular-weight chromium-binding substance? Polyhedron 16:4171–4177 (1997).
28. Davis MC, Royer AC, Vincent JB. Synthetic multinuclear chromium assembly activates insulin receptor kinase activity: functional model for low-molecular-weight chromium-binding substance. Inorg Chem 36:5316–5320 (1997).
29. Davis MC, Vincent JB. Isolation and characterization of a biologically active form of chromium oligopeptide from bovine liver. Arch Biochem Biophys 339:335–343 (1997).
30. Vincent JB. Mechanisms of chromium action: low-molecular-weight chromium-binding substance. J Am Coll Nutr 18:6–12 (1999).
31. Vincent JB. The biochemistry of chromium. J Nutr 130:715–718 (2000).
32. Vincent JB. Elucidating a biological role for chromium at a molecular level. Accounts Chem Res 33:503–510 (2000).
33. Speetjens JK, Collins RA, Vincent JB, Woski SA. The nutritional supplement chromium(III) tris(picolinate) cleaves DNA. Chem Res Toxicol 12:483–487 (1999).
34. Ellis T, Glass M, Harton A, Folting K, Huffman JC, Vincent JB. Synthetic models for low-molecular-weight chromium-binding substance: synthesis and characterization of oxo-bridged tetranuclear chromium(III) assemblies. Inorg Chem 33:5522–5527 (1994).
35. Sun Y, Ramirez J, Woski SA, Vincent JB. The binding of trivalent chromium to low-molecular-weight chromium-binding substance (LMWCr) and the transfer of chromium from transferring and $Cr(pic)_3$ to LMWCr. J Biol Inorg Chem 5:129–136 (2000).
36. Gaggelli E, Berti F, Gaggelli N, Maccotta A, Valensin G. A homodinuclear Cr(V)-Cr(V) complex forms from the chromate-glutathione reaction in water. J Am Chem Soc 123:8858–8859 (2001).
37. Jacobsen CJH, Pedersen E, Villadsen J, Weihe H. ESR characterization of *trans*-$V^{II}(py)_4X_2$ and *trans*-$Mn^{II}(py)_4X_2$ (X = NCS, Cl, Br, I; py = pyridine). Inorg Chem 32:1216–1221 (1993).
38. Lebedev YS. Very-high-field EPR and its applications. Appl Magn Reson 7:339–362 (1994).
39. Hypercube. Hyperchem, release 5.0. Reference manual. Waterloo, Ontario, CN:Hypercube Inc, 1997.
40. Brauer SL, Wetterhahn KE. Chromium(VI) forms a thiolate complex with glutathione. J Am Chem Soc 113:3001–3007 (1991).
41. Navon G, Valensin G. Nuclear relaxation times as a source of structural information. In: Metal Ions in Biological Systems, Vol 21 (Siegel H, ed). New York:Marcel Dekker, 1987;1–45.
42. Bertini I, Luchinat C. NMR of paramagnetic substances. Coord Chem Rev 150:29–110 (1996).
43. Solomon I. Relaxation processes in a system of two spins. Phys Rev 99:559–565 (1955).
44. Banci L, Bertini I, Luchinat C. Nuclear and Electron Relaxation. New York:VCH Publishers Inc,1991.